93-GHz Wireless Transmission enabled by a Wideband Photonic Oscillator based on two Phase-Locked Lasers

Antonio Malacarne
Photonic Networks & Technologies Nat'l Lab CNIT
Pisa, Italy
https://orcid.org/0000-0002-8240-2171

Alberto Montanaro
Photonic Networks & Technologies Nat'l Lab CNIT
Pisa, Italy
alberto.montanaro@cnit.it

Alessandra Bigongiari
Ericsson Research Ericsson
Pisa, Italy
alessandra.bigongiari@ericsson.com

Antonella Bogoni
Telecommunications, Computer Engineering, and Photonics Institute (TeCIP) Scuola Superiore Sant'Anna
Pisa, Italy
antonella.bogoni@santannapisa.it

Vito Sorianello
Photonic Networks & Technologies Nat'l Lab CNIT
Pisa, Italy
vito.sorianello@cnit.it

Claudio Porzi
Telecommunications, Computer Engineering, and Photonics Institute (TeCIP) Scuola Superiore Sant'Anna
Pisa, Italy
claudio.porzi@santannapisa.it

2024 International Topical Meeting on Microwave Photonics (MWP) | 979-8-3503-7539-8/24/$31.00 ©2024 IEEE | DOI: 10.1109/MWP62612.2024.10736221

***Abstract*—The mm-wave frequency spectrum offers the possibility to afford the increasing demand of high data-rate communication links. Microwave-photonics techniques can be advantageously used for reconfigurable generation of very high frequency clocks with no need for high-frequency and high-performance electrical oscillators and the additional functionality of remote distribution of the signal through fiber-optics or free-space optic links. Here we successfully test the spectral purity and stability of a wideband tunable photonic oscillator (WTPO) for supporting analog up-conversion of GHz-rate complex data signals in a W-band wireless transmission testbed. The oscillator output is derived from the beating into a photodiode of two narrow-linewidth lasers which are phase locked thanks to an electronic locking system. In this first demonstration, the WTPO output frequency has been multiplied to reach the target W band and error vector magnitude measurements attest the suitability of the solution for next generation 6G mobile networks.**

Keywords— Microwave photonics, mm-wave, 6G technology, sub-THz generation, wireless communications.

I. Introduction

The constant research for technological solutions to extend the transmission bandwidth of digital and analog signals concerns many applications including communication systems, radar sensors, and more. A larger bandwidth is required for sensing to achieve a better spatial resolution, whilst for telecommunications it translates in a higher information rate. The next 5G new radio (NR) and 6G wireless technologies are expected to afford the demand of high data-rate links and low-latency networks with maximized number of connected devices, to enable new applications such as digital twins, AI computing, remote surgery etc.[1]–[3]. In radio and wireless transmission systems, to enable larger signal bandwidth the carrier frequency needs to be increased, as well. The mm-wave frequency spectrum offers the possibility to meet the increasing demand of high data-rate communications links and corresponding higher carrier frequency. 6G is expected to be the first wireless technology to explore the use of sub-Terahertz (sub-THz) band frequencies in the range 100-300 GHz. Similarly, software defined radio receivers for military communications are also migrating in the V and W-band and, in addition to the increase of spatial resolution, civilian radar applications such as investigation of clouds and water moisture in the atmosphere require differential absorption measurements at 170 and 190 GHz [4]. In both remote sensing and transmission systems, the spectral purity of the employed carrier frequency, i.e. its frequency stability and phase noise (PN) performance, is crucial, impacting in the first case the maximum range and the capability to distinguish small targets [5], and in the latter the integrity of the transmitted data, especially when employing high-order modulation formats such as 256 quadrature amplitude modulation (QAM) or orthogonal frequency division multiplexing (OFDM) [6],[7]. As the operating frequency increases, standard electronics shows its limits in terms of PN and signal integrity [8]. For these reasons, microwave photonics techniques can be advantageously used to overcome these issues [9]. Sub-THz optical clocks obtained by heterodyning frequency combs into uni-travelling-carrier photodiodes with notable PN performance have been realized [10], and those type of implementations enable efficient clock distribution over low-loss and electromagnetic interference (EMI)-free fiber-optics or free-space optic links [11].

Recent results obtained by our research group are based on reconfigurable frequency multiplication of RF oscillations of a few tens of gigahertz, up to W-band and beyond, with PN performance in line with ideal frequency multipliers [12]–[14]. In this case, the degradation of noise is governed by $20\,log_{10}\,N$, being N the multiplication factor, and other technologies such as dielectric resonator oscillators (DROs), also exhibit limited spectral purity beyond Ka-band [15].

To overcome the limits imposed by frequency multiplication, together with achieving wideband tunability up to the millimeter–wave frequency bands, an ultra-wideband photonic oscillator capable of generating signals at frequencies as high as 110 GHz, with unprecedented low PN, has been recently introduced [15]. It is based on heterodyning, into a high-speed photodetector, two ultra-low noise semiconductor lasers spectrally spaced by the target frequency to be generated, each of them optically injection locked to an

The authors want to thank Miguel Maldonado (OEwaves, Inc.), Danny Eliyahu (OEwaves, Inc.) and Scott Singer (Comet Communication Systems, Inc.) for technical support and the use of both the oscillator prototype and the high-Q laser phase lock system.

ultra-high Q (> 10^9) crystalline optical whispering gallery mode (WGM) resonator [16]. In addition, the two narrow-linewidth (NLW) lasers have been embedded in an opto-electronic locking scheme including a phase-locked loop (PLL) to lock the frequency difference (and phase) of the two lasers to a reference low-frequency signal.

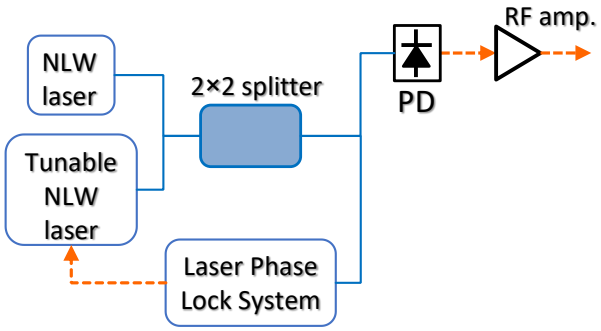

Fig. 1 Schematic diagram of the characterized and employed phase-locked wideband photonic oscillator.

Here, for the first time to the best of our knowledge, such a wideband tunable photonic oscillator (WTPO) is successfully used for analog up-conversion of GHz-rate quadrature phase-shift keying (QPSK) signals in a W-band wireless transmission testbed. A comprehensive characterization of the WTPO phase noise versus the generated frequency is included. A W-band optical clock is derived by the WTPO when operating in phase-locking regime, and employed for up-conversion and subsequent wireless transmission of QPSK signals up to 4 Gb/s. Error vector magnitude (EVM) performance attests the suitability of such approach for effective low-phase noise mm-wave band reference clock generation for B5G/6G mobile networks.

II. Characterization of the Wideband Tunable Photonic Oscillator

A complete characterization of the WTPO in terms of generated spectrum and corresponding phase noise power spectral density (PSD) up to 110 GHz is presented in ref. [15], in case of free run operation. Here, the performance of the device in case of phase-locked condition, is also going to be analyzed. To phase lock the two independent lasers, the setup in Fig. 1 has been used. Differently from [15], an electronic locking system (laser phase lock system, LPLS) that uses a

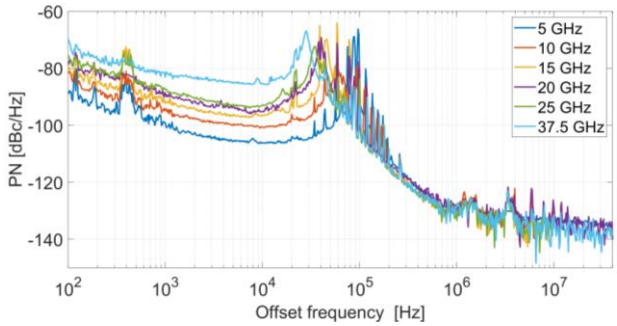

Fig. 2 Phase noise PSD of the generated electrical carrier for frequency ranging from 5 GHz t 37.5 GHz.

multiplied 100 MHz quartz oscillator to phase lock the two NLW lasers together, is employed [17]. After coupling the two laser outputs, half of the optical power is detected by a photodiode (PD) and amplified, whereas the other coupler output is delivered to the LPLS, whose output signal is used as feedback for adjusting the current of the tunable NLW laser cavity. The employed LPLS operating frequency is limited to 40 GHz, therefore the PN performance of the generated carrier frequency has been tested in the range 5–37.5 GHz, as reported in Fig. 2. From the comparison of the curves, it can be deduced that in the low offset frequency range (< 30–100 kHz) PN scales with f^2, as in case of frequency multiplication. Such behavior is consistent with the fact that for each target RF frequency, the multiplication factor of the 100 MHz quartz oscillator within the LPLS is consequently and automatically reconfigured. Thus, in this frequency range, the obtained PN is the one given by the quartz oscillator scaled at the target frequency within the locking bandwidth of the digital PLL included in the LPLS. On the other hand, in the high offset frequency range, the observed PN is independent of the generated frequency, as it only depends on the optical phase noise of the two NLW lasers, which does not change by tuning their emission frequency. Consequently, the calculated time jitter t_j for each curve in Fig. 2 is inversely proportional to the generated frequency [18]. As the generated frequency increases, the time jitter contribution due to the high offset range weights less and less, such that the total t_j eventually gets approximately constant and given by the behavior of each PN curve in the low offset range (calculated here to be about 46 fs). The calculated t_j versus the generated frequency is plotted in Fig. 3.

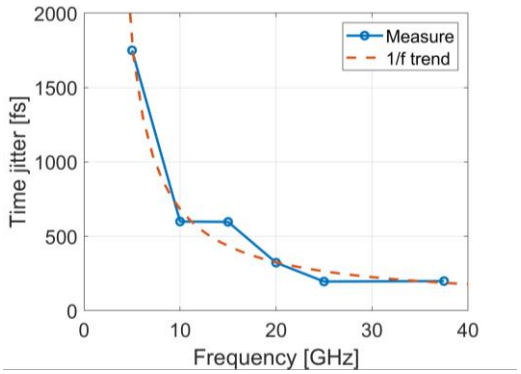

Fig. 3 Measured time jitter versus the generated carrier frequency, compared with a $1/f$ trend with asintotic value equal to 46 fs.

III. W-band Wireless Transmission Based on the Wideband Tunable Photonic Oscillator

Bands above 90 GHz are prime candidates for large volume applications in the backhaul and fronthaul to support all services requiring high speed wireless transmission. Standardization activities for the W-band (92 to 114.5 GHz) have been published in [19] and [20], with specific W-band allocation in the ITU Radio Regulation 2016 [21]. For all those reasons, the suitability of the proposed WTPO in phase-locked condition for W-band wireless transmission links has been verified in this work.

Since, as mentioned, the LPLS enables lasers' phase locking up to 40-GHz beating frequency, to reach the W-band frequency range a frequency multiplication of the WTPO electrical output is required. In this case, an 88-GHz optical clock is derived by fourfold frequency multiplication of a 22-GHz tone, generated by the WTPO when operating in phase-locking regime. The choice of the carrier frequency f_C =88 GHz is dictated by the available hardware used to implement the wireless transmission testbed, assuming an intermediate frequency (IF) f_{IF} =5 GHz for the data signal.

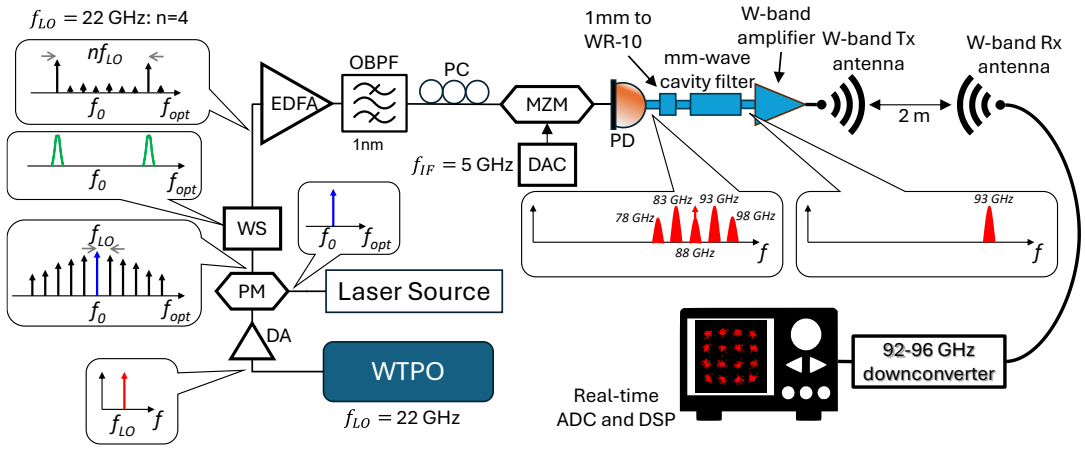

Fig. 4 Experimental setup for fourfold frequency multiplication of the WTPO output and W-band wireless transmission test.

To implement the fourfold 22-GHz frequency multiplication, a continuous-wave (CW) laser has been phase-modulated through a 40-GHz bandwidth electro-optic $LiNbO_3$ phase modulator (PM) driven by the WTPO output. An RF driver amplifier (DA) is used to boost the clock signal and induce a few-lines optical frequency comb (OFC) with 22-GHz line spacing at the PM output. A pair of 88 GHz-spaced modes out of the OFC are then selected using a commercial programmable optical waveshaper (WS) filter. A following Erbium-doped fiber amplifier (EDFA) compensates for device optical losses and a 1 nm-wide optical bandpass filter (OBPF) limits the out-of-band amplified spontaneous emission. An electro-optic $LiNbO_3$ Mach-Zehnder modulator (MZM) is then used to transfer the data signal on the two optical carriers. QPSK signals with baud rate ranging from 0.5 to 2 Gbaud (1–4 Gb/s) centered at f_{IF} have been generated by a 64 GS/s 11 GHz digital-to-analog converter (DAC). A polarization controller (PC) optimizes the MZM input polarization state. Fig. 5 shows the spectrum of the 88-GHz optical clock at both the input and output ports of the MZM, where the double sideband modulation of each optical carrier is notable. Fig. 6 reports the PN PSD of the native WTPO 22-GHz output frequency carrier together with the 88-GHz one obtained by photo-detecting the WS output. As expected in case of fourfold frequency multiplication, the comparison reveals a dBc/Hz difference of about 12 dB.

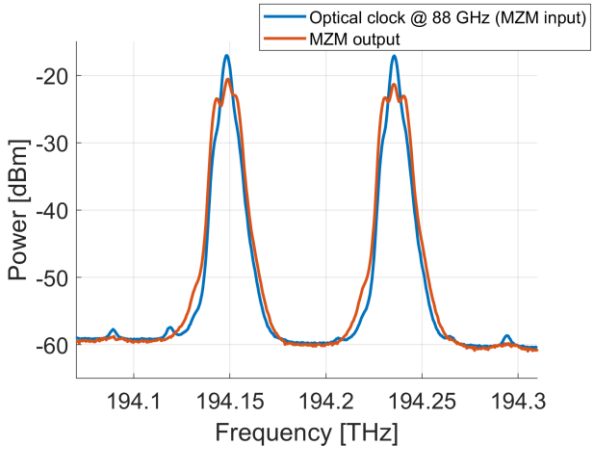

Fig. 5 Optical spectrum at the input and output of the MZM.

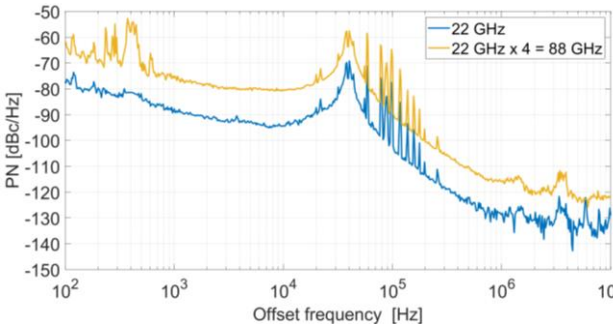

Fig. 6 Phase noise PSD of the generated 22-GHz electrical carrier compared with its fourfold frequency multiplied version at 88 GHz.

As shown in the setup of Fig. 4, the optical modulated signal is photo-detected by a 100-GHz PD. The subsequent hardware chain including a W-band filter with pass-band 86-94 GHz, W-band transmitting and receiving antennas and following commercial down-converter, all with operation bandwidth 92–96 GHz, leads to an effective 92–94 GHz transmission bandwidth, where the up-converted signal is centered ($f_C + f_{IF}$ =93 GHz). A 40 GS/s 12-GHz bandwidth real-time oscilloscope is finally used to acquire the signal and perform error vector magnitude (EVM) measurements.

The EVM performance of 1 Gb/s, 2 Gb/s and 4 Gb/s QPSK signal is detailed in Fig. 7 and has been measured through a digital signal processing (DSP) tool embedded in the oscilloscope. The DSP consists in phase recovery and in the use of an equalization filter whose length has been optimized in the range 21-51 symbols, depending on the modulation format and data rate. A digital raised cosine filter is also used, with bandwidth tailored according to the

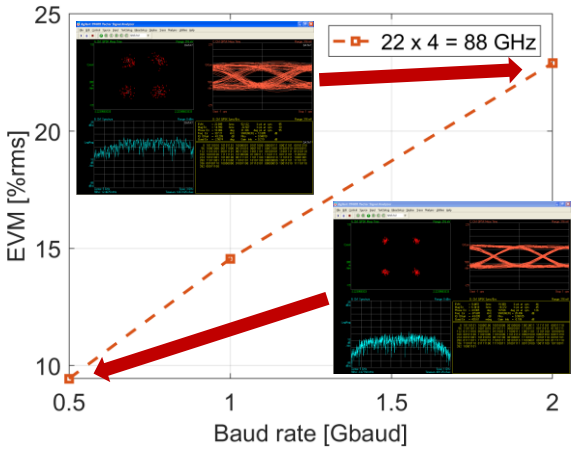

Fig. 7 Phase noise PSD of the generated 22-GHz electrical carrier compared with its fourfold frequency multiplied version at 88 GHz.

electrical bandwidth of the received signal. As shown by the two insets, the analysis also includes constellation reconstruction and visualization of I or Q eye diagram. With an optical power of 0 dBm at the PD input, an EVM = 9.4% was achieved at 1 Gb/s, observing a worsening up to 22.9% at 4 Gb/s. As expected, the performance degrades for higher data rate. The quite high penalty from 2 Gb/s to 4 Gb/s QPSK is most probably caused by the 2-GHz double-side bandwidth limitation imposed by the electrical chain of the employed W-band devices. In addition, the spectrum reported by the inset related to 2 Gb/s QPSK exhibits an asymmetric behavior (lower bound given by antennas and down-converter, upper bound given by the filter).

By comparing those results with previous similar ones obtained with the same testbed where the up-conversion process was achieved through an optoelectronic solution acting as an ideal frequency multiplier of a high-performance 20-GHz synthesizer output [12],[22], despite a significantly worse time jitter level, just a limited performance degradation has been observed here. Such result suggests that the major bottleneck in the system lies in the noise added during the electrical amplification and down-conversion of the data signal.

IV. Conclusions and Future Perspectives

A wideband tunable photonic oscillator embedding two separate laser sources has been characterized when operating is phase-locked regime. A commercial laser phase lock system, implementing an opto-electronic feedback loop for controlling the driving current of one of the two lasers, locks the beating frequency of the two lasers to that of a multiplied version of a lower frequency quartz oscillator output. The commercial system exhibits an operating range up to 40 GHz and provides, at its output, a control signal to feedback the cavity current of one of the two lasers.

A phase noise (PN) characterization of the system in the range of generated carrier frequency 5–37.5 GHz revealed a constant PN power spectral density for offset frequencies larger than a few tens of kHz, above which solely the contribution of the optical PN becomes relevant. For the lower offset frequency range, due to the digital PLL system, PN performance scales as in case of frequency multiplication.

The device has been successfully used for analog up-conversion of quadrature phase-shift keying (QPSK) signals with information rate up to 4 Gb/s, in a W-band wireless transmission testbed. EVM measurements confirm the effectiveness of the proposed phase-locked tunable photonic oscillator.

Future developments include a characterization of the receiver performance by using the approach shown here for signal down-conversion too. Another opportunity to improve the compactness of the system consists of replacing the optoelectronic modulation and photo-detection stages with the use of an optoelectronic photo-mixer, as in [23]. Finally, in addition to single-carrier PSK modulation formats, transmission performance of orthogonal frequency-division multiplexing (OFDM) signals will be investigated, to verify the suitability of the proposed solution with the requirements of current and forthcoming 5G, B5G and 6G standards.

References

[1] Cerwall, P. et al., "Ericsson Mobility Report November 2021", Ericsson Mobility Report 1–40, 2021

[2] S. Tripathi et al, "6G Mobile Wireless Networks", Springer (2021)

[3] X. You, CX. Wang, J. Huang et al. "Towards 6G wireless communication networks: vision, enabling technologies, and new paradigm shifts" Sci. China Inf. Sci. 64, 110301 (2021)

[4] R. J. Roy, K. B. Cooper, M. Lebsock, L. Millán, J. Siles and R. R. Monje, "Differential Absorption Radar at 170 GHz for Atmospheric Boundary Layer Water Vapor Profiling," 2018 15th European Radar Conference (EuRAD), Madrid, Spain, pp. 417-420, 2018

[5] M. Bauduin and A. Bourdoux, "Impact of Phase Noise on FMCW and PMCW Radars," 2023 IEEE Radar Conference, San Antonio, TX, USA, 2023, doi: 10.1109/RadarConf2351548.2023.10149598

[6]] A. G. Armada, "Understanding the effects of phase noise in orthogonal frequency division multiplexing (OFDM)," IEEE Transactions on Broadcasting, vol. 47, no. 2, pp. 153–159, Jun 2001.

[7] A. Leshem and M. Yemini, "Phase Noise Compensation for OFDM Systems," in IEEE Transactions on Signal Processing, vol. 65, no. 21, pp. 5675-5686, 1 Nov.1, 2017

[8] Rubiola, E. & Boudot, R., "Phase noise in RF and microwave amplifiers", 2010 IEEE International Frequency Control Symposium 109–111, 2010

[9] Sengupta, K., Nagatsuma, T. & Mittleman, D. M., "Terahertz integrated electronic and hybrid electronic–photonic systems", Nature Electronics 1, 622–635, 2018

[10] Tetsumoto, T. et al., "Optically referenced 300 GHz millimetre-wave oscillator", Nature Photonics 15 516–522, 2021

[11] A. Siligaris, Y. Andee, C. Jany, V. Puyal, J. M. Guerra, J.L.G. Jimenez, and P. Vincent, "A 270-to-300 GHz subharmonic injection locked oscillator for frequency synthesis in sub-mmW systems". IEEE Microwave and Wireless Components Letters, vol. 25, no. 4, pp.259-261, 2015

[12] A. Malacarne et al., "W-band Wireless Transmission based on 98 GHz Packaged Silicon Photonics Optical Clock Generator," 2024 Optical Fiber Communications Conference and Exhibition (OFC), San Diego, CA, USA, 2024, https://doi.org/10.1364/OFC.2024.M4J.6

[13] C. Porzi et al., "Spectrally Pure W-Band RF Carrier Generation with Packaged Silicon Photonics Circuit," in IEEE Journal of Quantum Electronics, doi: 10.1109/JQE.2024.3380552.

[14] A. Malacarne, A. Bigongiari, A. D'Errico, A. Bogoni and C. Porzi, "Reconfigurable Low Phase Noise RF Carrier Generation up to W-Band in Silicon Photonics Technology," in Journal of Lightwave Technology, vol. 40, no. 20, pp. 6891-6900, 15 Oct.15, 2022, doi: 10.1109/JLT.2022.3194361.

[15] D. Eliyahu et al., "Ultra-wideband Photonic VCO and Synthesizer," 2021 IEEE MTT-S International Microwave Symposium (IMS), Atlanta, GA, USA, 2021, pp. 538-540, doi: 10.1109/IMS19712.2021.9574828.

[16] W. Liang, V. S. Ilchenko, A. A. Savchenkov, A. B.Matsko, D. Seidel, and L. Maleki, "Whispering-gallerymode- resonator-based ultranarrow linewidth external cavity semiconductor laser," Opt. Lett., vol. 35, pp. 2822– 2824, August 2010

[17] https://www.oewaves.com/lock-box

[18] https://www.analog.com/media/en/training-seminars/tutorials/MT-008.pdf (last visit on July 8th, 2024)

[19] ECC Recommendation (18)02 of 14 September 2018 on radio frequency channel/block arrangements for Fixed Service systems operating in the bands 92-94 GHz, 94.1-100 GHz, 102-109.5 GHz and 111.8-114.25 GHz. Available at https://www.ecodocdb.dk/document/6037.

[20] ECC Report 282: "Point-to-Point Radio Links in the Frequency Ranges 92-114.25 GHz and 130-174.8 GHz", 2018. Available at https://www.ecodocdb.dk/document/6034.

[21] ITU-R Radio Regulation 2016. Available at https://www.itu.int/pub/R-REG-RR-2016.

[22] A. Montanaro et al., "93 GHz Wireless Transmission based on a Fully Packaged mm-Wave Band Optical Clock Generator," 2023 International Topical Meeting on Microwave Photonics (MWP), Nanjing, China, 2023, doi: 10.1109/MWP58203.2023.10416604

[23] A. Montanaro, G. Piccinini, V. Mišeikis et al., "Sub-THz wireless transmission based on graphene integrated optoelectronic mixer", 03 August 2022, PREPRINT (Version 1) available at Research Square [https://doi.org/10.21203/rs.3.rs-1835036